

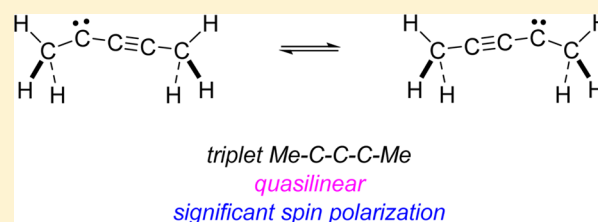
# Spectroscopy and Photochemistry of Triplet 1,3-Dimethylpropynylidene (MeC<sub>3</sub>Me)

Stephanie N. Knezz, Terese A. Waltz, Benjamin C. Haenni, Nicola J. Burrmann, and Robert J. McMahon\*

Department of Chemistry, University of Wisconsin-Madison, 1101 University Avenue, Madison, Wisconsin 53706-1322, United States

**S** Supporting Information

**ABSTRACT:** Photolysis ( $\lambda > 472$  nm) of 2-diazo-3-pentyne (**11**) affords triplet 1,3-dimethylpropynylidene (MeC<sub>3</sub>Me, **33**), which was characterized spectroscopically in cryogenic matrices. The infrared, electronic absorption, and electron paramagnetic resonance spectra of MeC<sub>3</sub>Me (**33**) are compared with those of the parent system (HC<sub>3</sub>H) to ascertain the effect of alkyl substituents on delocalized carbon chains of this type. Quantum chemical calculations (CCSD(T)/ANO1) predict an unsymmetrical equilibrium structure for triplet MeC<sub>3</sub>Me (**33**), but they also reveal a very shallow potential energy surface. The experimental IR spectrum of triplet MeC<sub>3</sub>Me (**33**) is best interpreted in terms of a quasilinear, axially symmetric structure. EPR spectra yield zero-field splitting parameters that are typical for triplet carbenes with axial symmetry ( $|D/hc| = 0.63$  cm<sup>-1</sup>,  $|E/hc| \sim 0$  cm<sup>-1</sup>), while theoretical analysis suggests that the methyl substituents confer significant spin polarization to the carbon chain. Upon irradiation into the near-UV electronic absorption ( $\lambda_{\text{max}}$  350 nm), MeC<sub>3</sub>Me (**33**) undergoes 1,2-hydrogen migration to yield pent-1-en-3-yne (**4**), a photochemical reaction that is typical of carbenes bearing a methyl substituent. This facile process apparently precludes photoisomerization to other interesting C<sub>5</sub>H<sub>6</sub> isomers, in contrast to the rich photochemistry of the parent C<sub>3</sub>H<sub>2</sub> system.



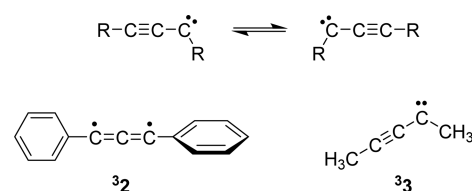
## INTRODUCTION

The study of acetylenic carbenes offers a deeper understanding of the electronic structure and chemical reactivity of conjugated carbon chain molecules. Propynylidene (HCCCH; **31**), the simplest acetylenic carbene, is an intermediate in reactions relevant to astrochemistry<sup>1,2</sup> and combustion of fuel-rich hydrocarbon flames.<sup>3,4</sup> The geometry and electronic structure of triplet propynylidene were once debated, but it is now generally accepted that **31** exists as a quasilinear species with C<sub>2</sub> equilibrium geometry (Scheme 1).<sup>5–8</sup> The electronic structure of **31** is best described as a nearly equal admixture of carbenic (1,1-diradical) and allenic (1,3-diradical) character (Scheme 1).<sup>7</sup>

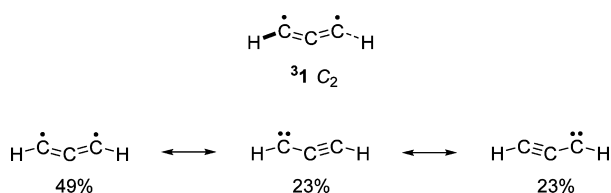
The case of triplet propynylidene notwithstanding, the study of acetylenic carbenes inevitably confronts the possibility of a localized carbene structure and the existence of bond-shift

isomers (Scheme 2). 1,3-Diphenylpropynylidene (PhC<sub>3</sub>Ph; **32**), the most carefully studied substituted derivative of propynylidene,

### Scheme 2



### Scheme 1<sup>a</sup>



<sup>a</sup>Equilibrium structure of **31** computed at CCSD(T)/cc-pVTZ; assessment of resonance contributors by Natural Resonance Theory at QCISD/6-311+G(2df,p).<sup>7</sup>

exhibits a symmetrical, allenic diradical structure with a triplet ground state.<sup>9</sup> In the current investigation, we describe experimental and computational studies of 1,3-dimethylpropynylidene (MeC<sub>3</sub>Me) (**33**). Although spectroscopic characterization (IR, UV/vis, and EPR) of MeC<sub>3</sub>Me (**33**) under matrix isolation conditions reveals many similarities to the parent HC<sub>3</sub>H system, theory predicts that symmetrical substitution of HC<sub>3</sub>H with two methyl substituents leads to an unsymmetrical, localized carbenic structure. The studies described herein answer some questions, and raise others, concerning the structure of triplet MeC<sub>3</sub>Me (**33**).

Received: July 19, 2016

Published: September 17, 2016

## RESULTS AND DISCUSSION

**Computational Results.** Relative energies of several pertinent  $C_5H_6$  isomers were computed using coupled-cluster and density functional theory methods. Coupled-cluster values (CCSD/cc-pVDZ) are provided in Figure 1. ( $T_1$  diagnostic

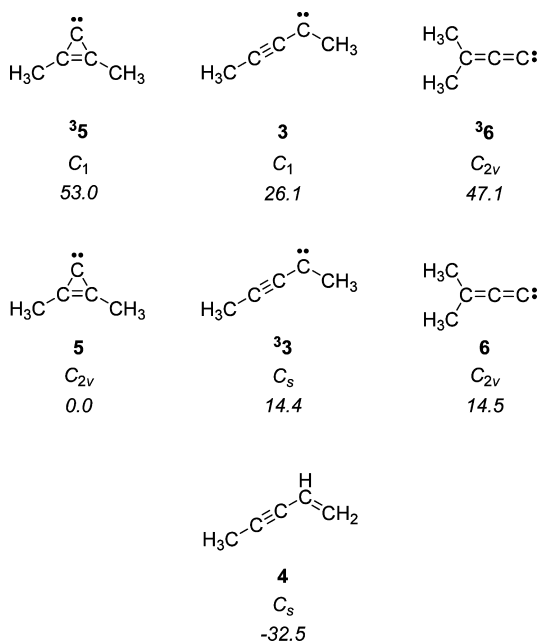


**Figure 1.** Computed relative energy (kcal/mol; CCSD/cc-pVDZ, including ZPVE) of selected  $C_5H_6$  isomers.

values, which may be used to assess the multi-reference character of the CCSD wave function,<sup>10,11</sup> are provided in Supporting Information.) DFT relative energies (B3LYP/6-31G(d)) are also provided in Supporting Information. Our computational data, involving both optimized structures and total electronic energies, exhibit poor agreement with the DFT data reported by Kassae and co-workers.<sup>12</sup> Geometry optimization of these systems is complicated because of the presence of two methyl rotors, and we surmise that this factor is responsible for the differences. In our study, we expended considerable effort to ensure that computed structures exhibit real vibrational frequencies (no imaginary frequencies) and thus represent true minima on the potential energy surface.

The relative energies of the dimethyl-substituted derivatives are qualitatively similar to those of the parent  $C_3H_2$  system. The major difference upon methyl substitution appears to be that singlets **5** and **6** experience a greater stabilization than triplet **3**. The computed energy separation between singlet 2,3-dimethylcyclopropenyliene (**5**) and triplet  $MeC_3Me$  (**3**) increases to 14.4 kcal/mol (from 9.8 kcal/mol for cyclopropenyliene vs triplet  $HC_3H$ ) while the separation between triplet  $MeC_3Me$  (**3**) and 3,3-dimethylpropadienyliene (**6**) decreases to 0.1 kcal/mol (from 3.4 kcal/mol for triplet  $HC_3H$  vs propadienyliene).<sup>6</sup>

The computed structures of triplet  $MeC_3Me$  (**3**) exhibit subtle differences that depend on the computational method and basis set employed (Figure 2). Density functional methods (B3LYP) predict a symmetrical delocalized structure ( $D_3$  symmetry) in which the deviation from an idealized  $D_{3d}$  structure varies with basis set (Figure 2a). (Huang et al. reported  $D_{3d}$  for the optimized structure at B3LYP/6-

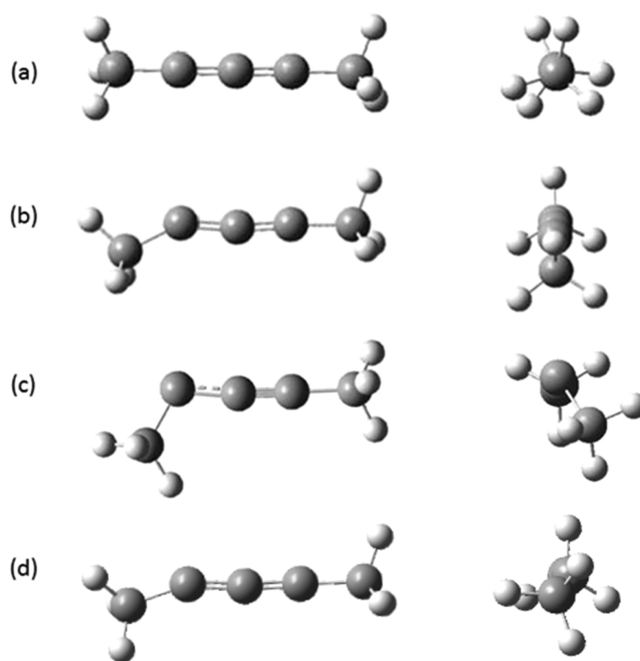
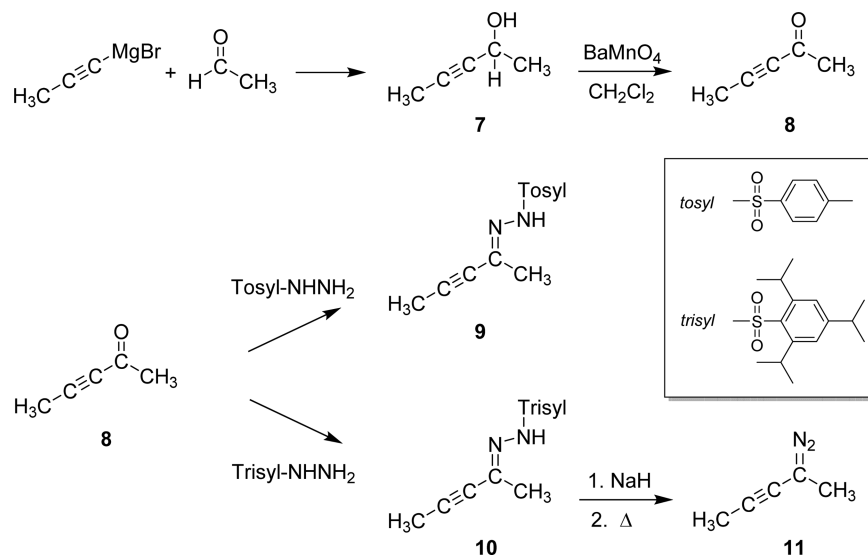


**Figure 2.** Computed structures for triplet and singlet  $MeC_3Me$  (**3**). (a)  ${}^33$  at B3LYP/6-31G(d) ( $D_3$ ). (b)  ${}^33$  at CCSD/cc-pVDZ ( $C_s$ ). (c)  ${}^13$  at CCSD/cc-pVDZ ( $C_1$ ). (d)  ${}^33$  at CCSD(T)/ANO1 ( $C_1$ ).

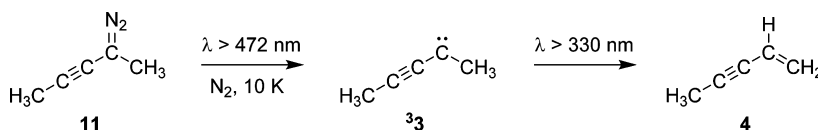
311G(d,p).<sup>13</sup>) Our DFT studies find that  $D_{3d}$  and  $D_{3h}$  structures each exhibit one imaginary vibrational frequency. At the CCSD/cc-pVDZ level, the carbon chain is bent and adopts an unsymmetrical, carbene-like structure in which the methyl groups are nonequivalent ( $C_s$  geometry) (Figure 2b). At the highest level of theory employed in this study (CCSD(T)/ANO1), a further distortion involving the dihedral angle of one of the methyl groups relative to the CCC plane removes all symmetry ( $C_1$  geometry) (Figure 2d). In contrast to these subtle complications associated with triplet  $MeC_3Me$  (**3**), the computed structure of singlet  $MeC_3Me$  (**13**) is less sensitive to the level of theory. At the CCSD/cc-pVDZ level, the structure of singlet  $MeC_3Me$  (**13**) is similar to the  $C_1$  structure obtained for triplet  $MeC_3Me$  (**3**), except for a more pronounced C–C–CH<sub>3</sub> angle at the “carbene” carbon ( $155^\circ$  in **3** vs  $114^\circ$  in **13**) (Figure 2c). The computed singlet–triplet energy splitting for  $MeC_3Me$  is 11.8 kcal/mol (CCSD/cc-pVDZ), which is quite similar to the experimentally measured value of 11.5 kcal/mol for the parent  $HC_3H$ .<sup>8</sup> The subtleties in structure for  $RC_3R$  systems make nomenclature challenging. The singlet and triplet states of  $MeC_3Me$  are each described by important resonance contributions from both carbene (propynylidene nomenclature: 1,3-dimethylpropynylidene or pent-3-yn-2-ylidene) and diradical (allene-diyl nomenclature: 1,3-dimethylallen-1,3-diyl or penta-2,3-dien-2,4-diyl) structures. For this reason, we often refer to the species by formula ( $MeC_3Me$ ) rather than by name.

**Carbene Precursor.** The preparation of 2-diazo-3-pentyne (**11**) was not as straightforward as we might have imagined. Pent-3-yn-2-one (**8**) was prepared according to literature procedures (Scheme 3).<sup>14,15</sup> Tosylhydrazone formation is occasionally problematic with simple ynals or ynones because of either conjugate addition or intramolecular cyclization of the initially formed tosylhydrazone to yield a pyrazole derivative.<sup>16,17</sup> In the current case, tosylhydrazone formation seemed to proceed normally, but subsequent treatment of the adduct with NaH under usual reaction conditions did not afford the

Scheme 3



Scheme 4



sodium salt. Although we were able to prepare the lithium salt of the tosylhydrazone with *n*-BuLi, thermolysis of the salt with matrix isolation trapping of the products afforded diazo compound **11** in low yield and impure form, as judged by the matrix IR spectrum. Thus, we turned to the preparation of the trisylhydrazone derivative—an approach that we employed in the related case of 1-diazo-1,3-diphenyl-2-propyne.<sup>9</sup> Gentle thermolysis of the sodium salt of trisylhydrazone **10** smoothly afforded 2-diazo-3-pentyne (**11**).

**Spectroscopy and Photochemistry of Me<sub>3</sub>Me (<sup>3</sup>3).** Photolysis ( $\lambda > 472$  nm) of 2-diazo-3-pentyne (**11**) under matrix isolation conditions (Ar or N<sub>2</sub>, 10 K) produces spectroscopic features attributable to triplet Me<sub>3</sub>Me (<sup>3</sup>3) (Scheme 4), as observed by IR, UV/vis, and EPR spectroscopy. Triplet Me<sub>3</sub>Me (<sup>3</sup>3) is photosensitive to near-UV irradiation ( $\lambda > 330$  nm), undergoing an intramolecular 1,2-hydrogen shift to produce pent-1-en-3-yne (**4**). In the following sections, we will discuss the details of the spectroscopic characterization of <sup>3</sup>3.

**IR Spectroscopy.** Photolysis ( $\lambda > 472$  nm, 6 h; N<sub>2</sub>, 10 K) of 2-diazo-3-pentyne (**11**) results in the disappearance of IR absorptions associated with the diazo compound and the appearance of new bands that can be attributed to triplet Me<sub>3</sub>Me (<sup>3</sup>3) (Figure 3). The new IR bands are inconsistent with those predicted for the diazine isomer of 2-diazo-3-pentyne (**11**) (Supporting Information). It should be noted that the computed IR spectra of triplet Me<sub>3</sub>Me (<sup>3</sup>3) presented in Figure 3 reflect not merely different levels of computational theory, they represent different predicted structures. The high symmetry structure (D<sub>3</sub>) predicted by B3LYP/6-31G(d) does not exhibit an IR-active C=C=C symmetric stretching vibration, while the low symmetry structure (C<sub>1</sub>) predicted by CCSD(T)/ANO1 does (1818 cm<sup>-1</sup>). Neither computational method takes into account the effects of anharmonicity. The unusually sharp peak at 1598 cm<sup>-1</sup> in the experimental

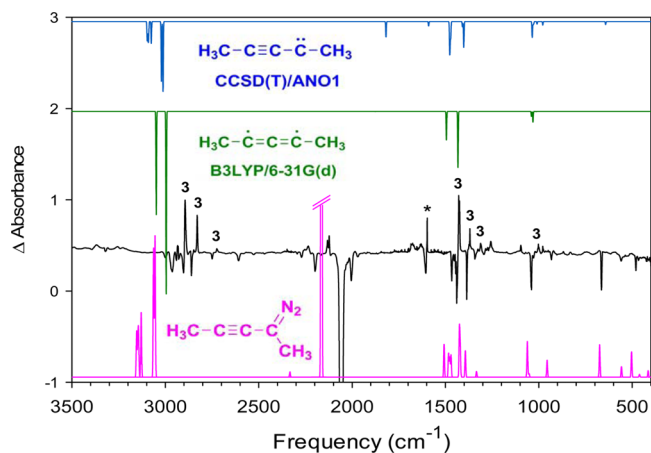


**Figure 3.** Top: Computed IR spectra for triplet Me<sub>3</sub>Me (<sup>3</sup>3) at CCSD(T)/ANO1 (above) and B3LYP/6-31G(d) (below). Middle: IR subtraction spectrum showing the disappearance of 2-diazo-3-pentyne (**11**) and appearance of triplet Me<sub>3</sub>Me (<sup>3</sup>3) upon irradiation ( $\lambda > 472$  nm, 6 h, N<sub>2</sub>, 10 K). Bottom: Computed spectrum for 2-diazo-3-pentyne (**11**) (CCSD/cc-pVDZ).

spectrum occurs in a region of the spectrum that is often contaminated by water. We are not confident in assigning this feature to triplet Me<sub>3</sub>Me (<sup>3</sup>3) and note that the agreement with the putative feature at 1818 cm<sup>-1</sup> in the predicted spectrum is much poorer than would be expected for a computation at this high level of theory. Thus, our tentative conclusion is that the absence of a C=C=C symmetric vibration in the IR spectrum of triplet Me<sub>3</sub>Me (<sup>3</sup>3) implies either a high-symmetry structure or a quasilinear molecular structure, in which degenerate unsymmetrical structures equilibrate because the barrier to linearity lies below the zero-

point energy. The parent  $\text{HC}_3\text{H}$  is experimentally known to be a quasilinear molecule.<sup>7,8</sup>

Subsequent irradiation ( $\lambda > 330$  nm, 24 h,  $\text{N}_2$ , 10 K) of the matrix containing triplet  $\text{MeC}_3\text{Me}$  ( $^3\mathbf{3}$ ) causes the disappearance of the IR absorptions associated with the triplet species and the appearance of new absorptions (Figure 4). The identity

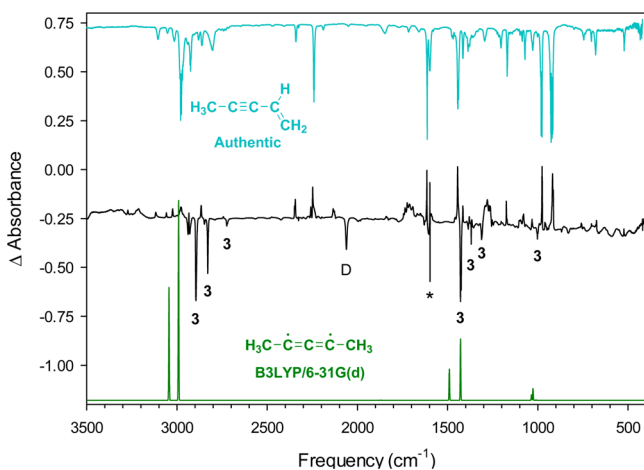


**Figure 4.** Top: Authentic IR spectrum of matrix isolated pent-1-en-3-yne ( $\mathbf{4}$ ) ( $\text{N}_2$ , 10 K). Middle: IR subtraction spectrum showing the disappearance of triplet  $\text{MeC}_3\text{Me}$  ( $^3\mathbf{3}$ ) and appearance of pent-1-en-3-yne ( $\mathbf{4}$ ) upon irradiation ( $\lambda > 330$  nm, 24 h,  $\text{N}_2$ , 10 K) (D = residual diazo compound  $\mathbf{11}$ ). Bottom: Computed IR spectrum of triplet  $\text{MeC}_3\text{Me}$  ( $^3\mathbf{3}$ ) (B3LYP/6-31G(d)).

of the photoproduct is assigned as pent-1-en-3-yne ( $\mathbf{4}$ ), the product of 1,2-hydrogen migration in  $\text{MeC}_3\text{Me}$ , by comparison with an IR spectrum of an authentic sample of enyne  $\mathbf{4}$ . To determine whether the 1,2-hydrogen shift reaction might also proceed via a tunneling mechanism, we allowed a matrix containing triplet  $\text{MeC}_3\text{Me}$  ( $^3\mathbf{3}$ ) to stand in the dark at 10 K. After 24 h, no changes were observed in the IR spectrum, thereby establishing that a hydrogen atom tunneling process is not operative.

**UV/vis Spectroscopy.** Photolysis ( $\lambda > 472$  nm, 11 h,  $\text{N}_2$ , 13 K) of 2-diazo-3-pentyne ( $\mathbf{11}$ ) results in bleaching of the strong UV absorption associated with the diazo compound ( $\lambda_{\text{max}}$  250 nm) and appearance of a weak near-UV absorption ( $\lambda_{\text{max}}$  350 nm) that can be attributed to triplet  $\text{MeC}_3\text{Me}$  ( $^3\mathbf{3}$ ) (Figure 5). The position and relative intensity of the electronic absorption of triplet  $\text{MeC}_3\text{Me}$  ( $^3\mathbf{3}$ ) is quite similar to that observed previously for triplet  $\text{HC}_3\text{H}$  ( $^3\mathbf{1}$ ), with the absorption of  $\text{MeC}_3\text{Me}$  ( $^3\mathbf{3}$ ) exhibiting a slight redshift ( $\lambda_{\text{max}}$  350 nm vs 310 nm).<sup>6</sup> In analogy to the behavior observed in the IR experiments, photoexcitation ( $\lambda > 330$  nm, 3 h) into the near-UV electronic absorption ( $\lambda_{\text{max}}$  350 nm) of triplet  $\text{MeC}_3\text{Me}$  ( $^3\mathbf{3}$ ) results in efficient bleaching of the absorption of  $^3\mathbf{3}$  and the appearance of a strong UV absorption attributable to pent-1-en-3-yne ( $\mathbf{4}$ ), the product of 1,2-hydrogen migration (Figure 5). When a matrix containing triplet  $\text{MeC}_3\text{Me}$  ( $^3\mathbf{3}$ ) was allowed to stand in the dark for 24 h, no changes occurred in the electronic absorption spectrum.

**EPR Spectroscopy.** Photolysis ( $\lambda > 613$  nm, 13.75 h; Ar, 10 K) of 2-diazo-3-pentyne ( $\mathbf{11}$ ) affords the triplet EPR spectrum of  $\text{MeC}_3\text{Me}$  ( $^3\mathbf{3}$ ) (Figure 6). The appearance of two sets of signals in the EPR spectrum (major and minor) could be a result of a matrix site effect or the presence of distinct conformational isomers. An axially symmetric structure for

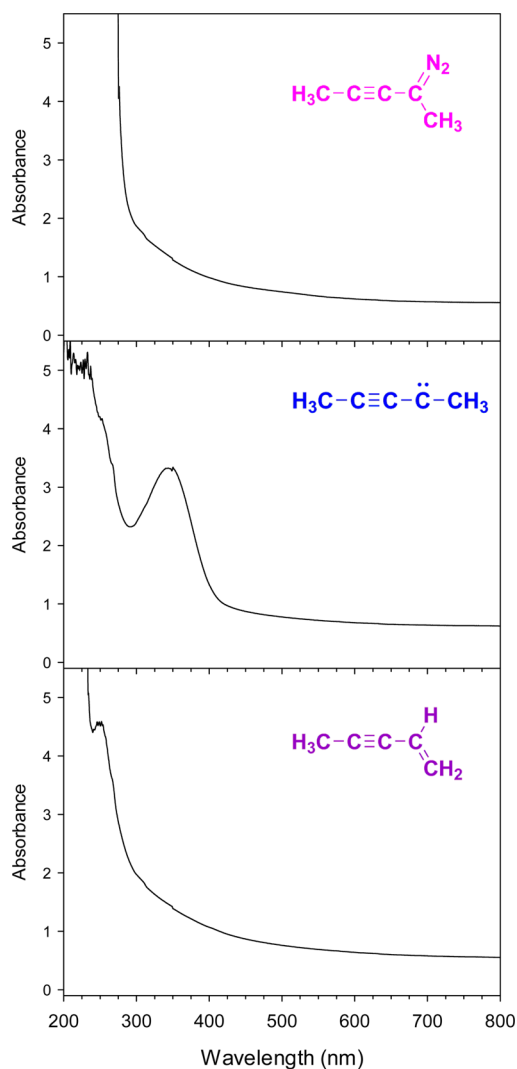


**Figure 5.** Top: Electronic absorption spectrum of 2-diazo-3-pentyne ( $\mathbf{11}$ ) after deposition (60 min,  $\text{N}_2$ , 13 K). Middle: Triplet  $\text{MeC}_3\text{Me}$  ( $^3\mathbf{3}$ ) obtained upon irradiation of  $\mathbf{11}$  ( $\lambda > 472$  nm, 11 h). Bottom: Pent-1-en-3-yne ( $\mathbf{4}$ ) obtained upon irradiation of  $^3\mathbf{3}$  ( $\lambda > 330$  nm, 3 h).

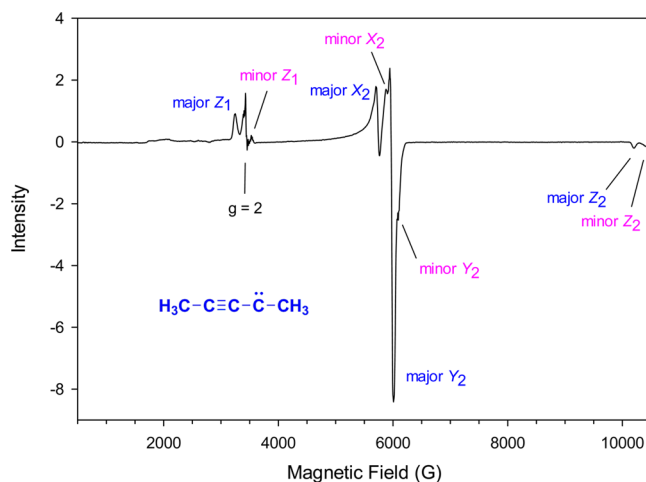


**Figure 6.** EPR spectrum of triplet  $\text{MeC}_3\text{Me}$  ( $^3\mathbf{3}$ ) after irradiation of 2-diazo-3-pentyne ( $\mathbf{11}$ ) ( $\lambda > 613$  nm, 13.75 h; Ar, 10 K).

MeC<sub>3</sub>Me (<sup>3</sup>3) should exhibit a single XY<sub>2</sub> transition rather than distinct X<sub>2</sub> and Y<sub>2</sub> transitions. That being said, the deviation from axial symmetry is not large. The issues of matrix effects and relaxed vs nonrelaxed structures have been dealt with, in considerable detail, for the closely related cases of HC<sub>3</sub>H (<sup>3</sup>1)<sup>7</sup> and PhC<sub>3</sub>Ph (<sup>3</sup>2).<sup>9</sup>

The values of the zero-field splitting parameter *D* (major: |*D*/*hcl* = 0.627 cm<sup>-1</sup>; minor: 0.651 cm<sup>-1</sup>) are comparable to the parent HC<sub>3</sub>H (|*D*/*hcl* = 0.64 cm<sup>-1</sup>),<sup>6,7</sup> indicating that alkyl substituents do not greatly affect the spin density of the π system. A similar relationship was observed among the triplets HC<sub>5</sub>H, MeC<sub>5</sub>H, and MeC<sub>5</sub>Me.<sup>18</sup> While the large *D* value might seem to favor a carbenic structure rather than a 1,3-allenic diradical structure, it is now understood that one-center dipolar couplings of the unpaired spins at the C-1 and C-3 positions of the carbon chain give rise to large *D* values in systems of this type.<sup>7</sup> The very small values of the zero-field splitting parameter *E* (major: |*E*/*hcl* = 0.0073 cm<sup>-1</sup>; minor: 0.0048 cm<sup>-1</sup>) are consistent with small deviations from axial symmetry—whether they be intrinsic to the structure or imposed by subtle perturbations of the host matrix.

Subsequent irradiation ( $\lambda > 299$  nm) of the matrix containing triplet MeC<sub>3</sub>Me (<sup>3</sup>3) causes a substantial decrease of the triplet signal, consistent with the photoisomerization of MeC<sub>3</sub>Me (<sup>3</sup>3) to pent-1-en-3-yne (4). No new triplet EPR transitions were observed in subsequent irradiations at shorter wavelengths.

**Structure.** Prior experimental<sup>6,7,19,20</sup> and theoretical studies<sup>21,22</sup> establish symmetrical structures for HC<sub>3</sub>H, HC<sub>5</sub>H, and HC<sub>7</sub>H. That symmetrical disubstitution of the symmetrical HC<sub>3</sub>H (1) would result in an unsymmetrical structure for MeC<sub>3</sub>Me (3) came as an unexpected result to us. For the first time, we seem to have stumbled into an acetylenic carbene that favors an unsymmetrical structure. If the molecule is indeed unsymmetrical, then there must be two equivalent unsymmetrical structures (bent at one end or the other) (Figure 7).

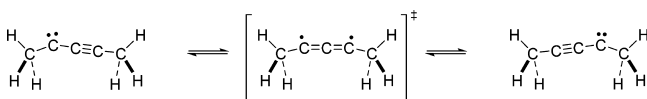


**Figure 7.** Qualitative depiction of putative automerization process in triplet MeC<sub>3</sub>Me (<sup>3</sup>3). CCSD/cc-pVDZ structure is C<sub>s</sub> symmetry.

The atomic motion required to transform one structure into the other is very small. Thus, the putative barrier cannot be very large. We searched the potential energy surface diligently, but without success, to find a transition state between these two equivalent structures. As a measure of assessing the flatness of the potential energy surface, we performed geometry optimizations at the CCSD(T)/ANO1 level under the constraint of *D*<sub>3</sub>, *D*<sub>3h</sub>, or *D*<sub>3d</sub> symmetry. In each case, the structures exhibit five imaginary vibrational frequencies (two doubly degenerate bends and one stretch), establishing that the computed energies of these structures represent upper limits for actual low-energy transition states on the potential energy surface. The *D*<sub>3</sub>, *D*<sub>3h</sub>, and *D*<sub>3d</sub> structures are exceedingly close in energy to the fully optimized C<sub>1</sub> structure (unsymmetrical carbene), lying only 0.2 kcal/mol (70 cm<sup>-1</sup>) higher than the C<sub>1</sub> structure (Table 1). Upon inclusion of zero-point vibrational energy, the relative energies actually reverse; the high symmetry structures lie 0.4 kcal/mol lower in energy than the C<sub>1</sub> structure. These calculations demonstrate that triplet

**Table 1.** Computed Energies for Triplet MeC<sub>3</sub>Me (<sup>3</sup>3)<sup>a</sup>

| symmetry        | N(i) <sup>b</sup> | E <sup>c</sup> | E (rel) <sup>d</sup> | E + ZPVE <sup>c</sup> | E + ZPVE (rel) <sup>d</sup> |
|-----------------|-------------------|----------------|----------------------|-----------------------|-----------------------------|
| C <sub>1</sub>  | 0                 | -193.626328    | 0.00                 | -193.541322           | 0.00                        |
| D <sub>3</sub>  | 5                 | -193.626001    | 0.21                 | -193.541975           | -0.41                       |
| D <sub>3h</sub> | 5                 | -193.626000    | 0.21                 | -193.541975           | -0.41                       |
| D <sub>3d</sub> | 5                 | -193.626003    | 0.20                 | -193.541573           | -0.16                       |

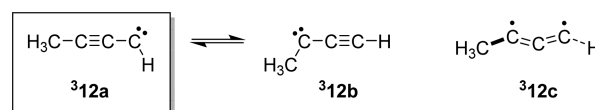
<sup>a</sup>CCSD(T)/ANO1; *D*<sub>3</sub>, *D*<sub>3h</sub>, *D*<sub>3d</sub> geometry optimizations constrained to the given symmetry. <sup>b</sup>Number of imaginary vibrational frequencies. <sup>c</sup>Total energy in Hartree. <sup>d</sup>Relative energy in kcal/mol.

MeC<sub>3</sub>Me (<sup>3</sup>3) resides on an exceptionally shallow portion of the potential energy surface. They also underscore the challenge of understanding these subtle features in detail. It is likely that this system is not well treated within the harmonic approximation and it is possible that it is not well treated with the Born–Oppenheimer approximation.<sup>23</sup>

On the basis of the flat potential energy surface and the very low frequency vibrational mode (8 cm<sup>-1</sup>, B3LYP/6-31G(d); 9 cm<sup>-1</sup>, CCSD(T)/ANO1), as well as by analogy with related systems,<sup>7,8,24</sup> we infer that triplet MeC<sub>3</sub>Me (<sup>3</sup>3) is a quasilinear molecule.<sup>25–29</sup> This inference lends support to the interpretation of the IR spectrum, as described above. Even though a sophisticated electronic structure calculation predicts an unsymmetrical equilibrium structure for triplet MeC<sub>3</sub>Me (<sup>3</sup>3), the flatness of the potential energy surface affords a quasilinear structure. Thus, the experimental IR spectrum of triplet MeC<sub>3</sub>Me (<sup>3</sup>3) is best described by in terms of a higher symmetry structure (*D*<sub>3</sub>) and not the predicted, low-symmetry equilibrium structure (C<sub>1</sub>).

Puzzled by the result that symmetrical disubstitution of the C<sub>2</sub>-symmetric HC<sub>3</sub>H (1) with methyl substituents gives rise to an unsymmetrical structure for MeC<sub>3</sub>Me (3), we attempted to dissect the problem by considering the influence of substituting HC<sub>3</sub>H (1) with a single methyl group (Scheme 5). Triplet

**Scheme 5**



MeC<sub>3</sub>H (<sup>3</sup>12) has been the subject of occasional interest through the years. The triplet EPR spectrum ascribed to MeC<sub>3</sub>H (<sup>3</sup>12a) was reported by Bernheim, Skell, and co-workers in the 1960s.<sup>30,31</sup> More recently, MeC<sub>3</sub>H (<sup>3</sup>12a) has been characterized as quasilinear by theoretical methods.<sup>32</sup> Computed structures (DFT) have been reported for <sup>3</sup>12a,<sup>32,33</sup> but attempts to obtain a geometry-optimized structure for the bond-shift isomer, <sup>3</sup>12b, converged to <sup>3</sup>12a.<sup>33</sup> In our current studies, we replicated these computational results at both DFT and coupled-cluster levels of theory. With respect to the effect of methyl substitution in triplet HC<sub>3</sub>H, the first methyl substituent appears to exert the dominant effect in biasing the system in favor of the alkynyl-substituted propargylic structure MeC≡CCH (<sup>3</sup>12a). A structure in which the first methyl substituent is at the carbenic position MeCC≡CH (<sup>3</sup>12b) is not only higher in energy than <sup>3</sup>12a, <sup>3</sup>12b is not even a minimum on the potential energy surface. In MeC<sub>3</sub>Me (<sup>3</sup>3), the second methyl substituent is forced to occupy the less energetically favorable carbenic position. We scoured the electronic structure calculations and natural bond orbital

(NBO) analyses of these systems for insights into the nature of these subtle interactions, but we were unable to identify dominant interactions on this very shallow potential energy surface.

As noted in the Introduction, one of the fascinating characteristics of the electronic structure of triplet  $\text{HC}_3\text{H}$  ( $^3\mathbf{1}$ ) is the nearly equal admixture of carbenic (1,1-diradical) and allenic (1,3-diradical) character. Figure 8 presents a comparison

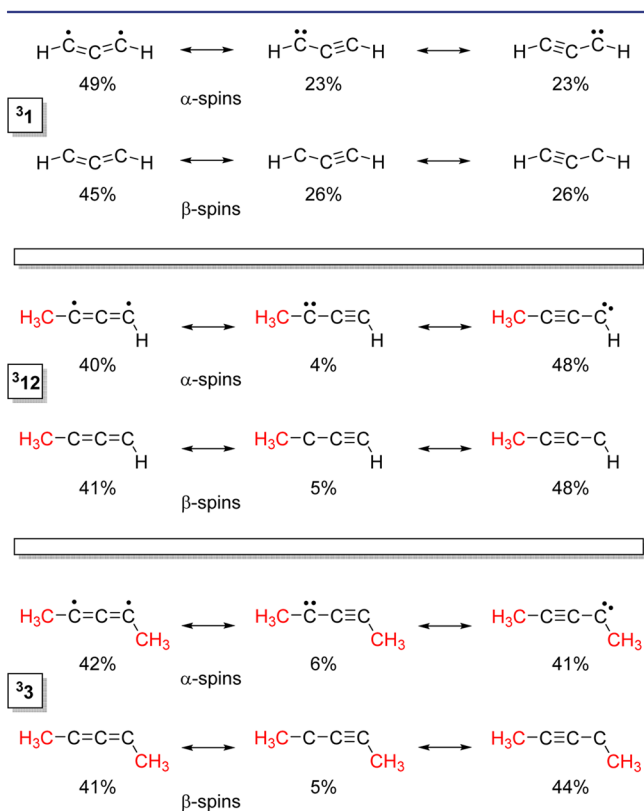


**Figure 8.** Natural resonance theory (NRT) descriptions of triplets  $\text{HC}_3\text{H}$  ( $^3\mathbf{1}$ ),  $\text{MeC}_3\text{H}$  ( $^3\mathbf{12}$ ), and  $\text{MeC}_3\text{Me}$  ( $^3\mathbf{3}$ ). ( $^3\mathbf{1}$ , QCISD/6-311+G(2df,p);  $^3\mathbf{12}$ , CCSD(T)/cc-pVTZ//CCSD/cc-pVDZ;  $^3\mathbf{3}$ , CCSD(T)/cc-pVTZ//CCSD(T)/ANO1).

of the natural resonance theory/natural bond orbital analyses for the triplets  $\text{HC}_3\text{H}$  ( $^3\mathbf{1}$ ),  $\text{MeC}_3\text{H}$  ( $^3\mathbf{12}$ ), and  $\text{MeC}_3\text{Me}$  ( $^3\mathbf{3}$ ). Although the influence of one or two methyl substituents is not dramatic, the effects are a modest enhancement of carbenic character of  $\text{HC}_3\text{H}$  ( $^3\mathbf{1}$ ).

NBO analyses also provide insight concerning spin densities and electron delocalization along the carbon chain in these systems. Our earlier analysis of triplet  $\text{HC}_3\text{H}$  ( $^3\mathbf{1}$ ) revealed the existence of significant spin polarization along the carbon backbone, which turned out to be a crucial insight in developing a suitable rationalization for the magnitude of the zero-field splitting parameter,  $D$ .<sup>7</sup> In the current study, the degree to which methyl substitution enhances the spin polarization, relative to  $\text{HC}_3\text{H}$  ( $^3\mathbf{1}$ ), came as a surprise because the effect of methyl substitution was not pronounced in our earlier study of triplets  $\text{HC}_5\text{H}$  vs  $\text{MeC}_5\text{H}$ .<sup>19,34</sup> Natural spin densities ( $\rho$ ) for triplets  $\text{HC}_3\text{H}$  ( $^3\mathbf{1}$ ),  $\text{MeC}_3\text{H}$  ( $^3\mathbf{12}$ ), and  $\text{MeC}_3\text{Me}$  ( $^3\mathbf{3}$ ) are presented in Table 2. Of particular note is the substantial increase in negative spin density at the center carbon of the chain upon substitution by one or two methyl groups (from  $\rho = -0.40$  in  $\text{HC}_3\text{H}$  to  $\rho = -0.98$  in  $\text{MeC}_3\text{H}$ ). The effects of two methyl substituents are not additive and

**Table 2.** Computed Spin Densities for Triplets  $\text{HC}_3\text{H}$  ( $\mathbf{1}$ ),  $\text{MeC}_3\text{H}$  ( $\mathbf{12}$ ), and  $\text{MeC}_3\text{Me}$  ( $\mathbf{3}$ )<sup>a</sup>

| atom                     | natural spin density                   |  |  |
|--------------------------|--|--|--|
|                          | $\text{HC}_3\text{H}$ ( $\mathbf{1}$ ) | $\text{MeC}_3\text{H}$ ( $\mathbf{12}$ ) | $\text{MeC}_3\text{Me}$ ( $\mathbf{3}$ ) |
| H-1                      |  | 0.04                                     | 0.04                                     |
| H-2                      |  | 0.04                                     | 0.05                                     |
| H-3                      |  | 0.04                                     | 0.04                                     |
| C- $\alpha$              |  | -0.14                                    | -0.14                                    |
| H                        | -0.04                                  |  |  |
| C-1                      | 1.24                                   | 1.36                                     | 1.38                                     |
| C-2                      | -0.40                                  | -0.98                                    | -0.93                                    |
| C-3                      | 1.24                                   | 1.70                                     | 1.57                                     |
| H                        | -0.04                                  | -0.07                                    |  |
| C- $\beta$               |  |  | -0.14                                    |
| H-4                      |  |  | 0.03                                     |
| H-5                      |  |  | 0.05                                     |
| H-6                      |  |  | 0.05                                     |
| $\Sigma$ (lspin density) | 2.96                                   | 4.37                                     | 4.42                                     |
| $\Sigma$ (spin density)  | 2.00                                   | 1.99                                     | 2.00                                     |
| "excess" spin density    | 0.96                                   | 2.38                                     | 2.42                                     |

<sup>a</sup>From the natural bond orbital (NBO) analyses of triplets  $\text{HC}_3\text{H}$  ( $^3\mathbf{1}$ ) QCISD/6-311+G(2df,p),<sup>7</sup>  $\text{MeC}_3\text{H}$  ( $^3\mathbf{12}$ ) CCSD(T)/cc-pVTZ//CCSD/cc-pVDZ, and  $\text{MeC}_3\text{Me}$  ( $^3\mathbf{3}$ ) CCSD(T)/cc-pVTZ//CCSD(T)/ANO1).

appear to be dominated by the first methyl group, which enforces the alkynyl-substituted propargylic structure, as noted earlier. Systems displaying significant spin polarization may be considered to have spin density in "excess" of the spin density formally associated with the number of unpaired electrons.<sup>35</sup> For the triplet species under consideration, there are two unpaired electrons and the arithmetic sum of the spin density,  $\Sigma$  (spin density) affords the expected value of  $\rho = 2.0$ . Because of spin polarization, the sum of the absolute values of the spin densities at each atom,  $\Sigma$  (lspin density), exceeds the formal spin density by a considerable magnitude. For  $\text{HC}_3\text{H}$  ( $^3\mathbf{1}$ ), the "excess" spin density is  $\rho = 0.96$ , while for  $\text{MeC}_3\text{H}$  ( $^3\mathbf{12}$ ), it is  $\rho = 2.38$ , and for  $\text{MeC}_3\text{Me}$  ( $^3\mathbf{3}$ ) it is  $\rho = 2.42$  (Table 2). Thus, the calculations predict that the introduction of a single methyl group in triplet  $\text{HC}_3\text{H}$  ( $^3\mathbf{1}$ ) enhances the spin polarization by an amount greater than one full electron. The concept of spin polarization is not merely a theoretical construct; the consequences are subject to experimental verification, as has been done in the case of triplet  $\text{HC}_3\text{H}$  ( $^3\mathbf{1}$ ).<sup>7</sup>

**Photochemistry.** The family of structures on the  $\text{C}_3\text{H}_2$  potential energy surface exhibits a rich network of photoisomerization reactions,<sup>6</sup> many of which involve hydrogen migration. In the phenyl-substituted series ( $\text{C}_3\text{Ph}_2$ ), the analogous migration reactions of phenyl substituents are not observed, but the photocyclization reaction of triplet  $\text{PhC}_3\text{Ph}$  to form singlet 2,3-diphenylcyclopropenyldiene still occurs.<sup>9</sup> In analyzing our IR data involving the photochemistry of  $\text{MeC}_3\text{Me}$  ( $^3\mathbf{3}$ ), we checked for the formation of 2,3-dimethylcyclopropenyldiene ( $\mathbf{5}$ ) but found none. Photoexcitation ( $\lambda > 330$  nm, 3 h) into the near-UV electronic absorption ( $\lambda_{\text{max}}$  350 nm) of triplet  $\text{MeC}_3\text{Me}$  ( $^3\mathbf{3}$ ) affords 1,2-hydrogen migration, to form pent-1-en-3-yne ( $\mathbf{4}$ ), as the dominant photochemical process. This mode of photochemical reactivity has also been observed

with  $\text{MeC}_5\text{H}_3$ ,<sup>34</sup>  $\text{MeC}_5\text{Me}$ ,<sup>18</sup> and  $\text{MeC}_7\text{H}$ .<sup>20</sup> We explored broad range of irradiation wavelengths in the study of triplet  $\text{MeC}_3\text{Me}$  (**3**), but no additional photoproducts were observed.

## CONCLUSIONS

Triplet carbene  $\text{MeC}_3\text{Me}$  (**3**) has been generated under matrix isolation conditions by photolysis of 2-diazo-3-pentyne (**11**) in  $\text{N}_2$  and characterized by IR, UV/vis, and EPR spectroscopy. Although quantum chemical calculations predict an unsymmetrical equilibrium structure, they also reveal a shallow potential energy surface. The experimental IR spectrum of triplet  $\text{MeC}_3\text{Me}$  (**3**) is best interpreted in terms of a quasilinear, axially symmetric structure. Theoretical analysis of the electronic structure of this intriguing molecule suggests that the methyl substituents confer significant spin polarization to this small, open-shell, carbon-chain molecule.

## EXPERIMENTAL SECTION

**General.** Chemicals and solvents were purchased and used without purification, unless otherwise noted.  $^1\text{H}$  NMR spectra (300 or 400 MHz) and  $^{13}\text{C}$  NMR spectra (75.4 MHz) were obtained in  $\text{CDCl}_3$ ; chemical shifts ( $\delta$ ) are reported as ppm downfield from internal  $\text{SiMe}_4$ . Mass spectra were acquired using a high-performance liquid chromatography electrospray ionization quadrupole mass spectrometer.

**Computational Methods.** Equilibrium geometries, harmonic vibrational frequencies, and infrared intensities were computed using density functional or coupled-cluster methods. Density functional calculations were performed using the B3LYP functional and the 6-31G(d) basis set, as implemented in the Gaussian 09 program suite.<sup>36</sup> Coupled-cluster calculations were performed at CCSD or CCSD(T) levels with the cc-pVDZ or ANO1 basis sets, as implemented in the CFOUR program suite.<sup>37</sup> NBO and NRT calculations<sup>38</sup> were performed as implemented in the Gaussian program suite.

**Pent-3-yn-2-ol (7).**<sup>14</sup> 1-Propynyl magnesium bromide (100 mL, 50 mmol) was concentrated at reduced pressure to approximately 50 mL, purged with nitrogen, and cooled to 0 °C. A solution of freshly distilled and dried acetaldehyde (6 mL, 105 mmol) in 40 mL anhydrous diethyl ether was added dropwise via syringe under nitrogen at 0 °C. The flask was warmed to room temperature and allowed to stir under nitrogen. After 5 h, the reaction was quenched by addition of 60 mL saturated ammonium chloride solution. The white precipitate was removed by vacuum filtration. The aqueous layer of the resulting biphasic solution was extracted twice with diethyl ether. The combined organic layers were washed with water, followed by brine. The ether solution was dried over  $\text{MgSO}_4$ , filtered, and concentrated at reduced pressure to reveal a yellow oil. The crude product was distilled at reduced pressure to afford pent-3-yn-2-ol (**7**) (2.58 g, 30.7 mmol, 61%).  $^1\text{H}$  NMR (300 MHz,  $\text{CDCl}_3$ ):  $\delta$  4.50 (qq,  $J = 6.6, 2.1$  Hz, 1H), 2.46 (s, br, 1H), 1.84 (d,  $J = 2.1$  Hz, 3H), 1.42 (d,  $J = 6.6$  Hz, 3H).

**Pent-3-yn-2-one (8).**<sup>39</sup> To a flame-dried 100 mL round-bottom flask were added 20 mL dry  $\text{CH}_2\text{Cl}_2$ , 6.55 g  $\text{BaMnO}_4$  (25.6 mmol), and 1.20 mL 3-pentyn-2-ol (**7**) (12.8 mmol). The mixture was allowed to stir under nitrogen at room temperature overnight. The mixture was filtered through a medium fritted funnel to remove  $\text{BaMnO}_4$ , and the solution was concentrated under reduced pressure to reveal pent-3-yn-2-one (**8**) (0.76 g, 9.27 mmol, 72% yield) as a gold oil. No purification was necessary.  $^1\text{H}$  NMR (300 MHz,  $\text{CDCl}_3$ ):  $\delta$  2.31 (s, 3H), 2.02 (s, 3H).  $^{13}\text{C}$  NMR ( $\text{CDCl}_3$ ): 184.9, 90.1, 80.6, 32.9, 4.1.

**Pent-3-yn-2-one Tosylhydrazone (9).** To a flask containing 0.76 g (9.23 mmol) pent-3-yn-2-one (**8**) was added 7.0 mL glacial acetic acid and 2.80 g (15.1 mmol) tosylhydrazide. The mixture was allowed to stir under nitrogen at room temperature overnight. The mixture was poured into a beaker containing 100 mL of saturated sodium bicarbonate solution, stirred for 15 min, and poured into a separatory funnel containing dichloromethane and water. The organic layer was

dried with anhydrous magnesium sulfate, filtered, concentrated under reduced pressure, and purified using flash column chromatography ( $\text{CHCl}_3$ ). Concentration of the appropriate fractions revealed pent-3-yn-2-one tosylhydrazone (**9**) (1.24 g, 4.93 mmol, 53%) as a white powder.  $^1\text{H}$  NMR (300 MHz,  $\text{CDCl}_3$ ):  $\delta$  8.61 (s, 1H), 7.84 (d,  $J = 8.0$  Hz, 2H), 7.30 (d,  $J = 8.0$  Hz, 2H), 2.40 (s, 3H), 2.05 (s, 3H), 1.99 (s, 3H).  $^{13}\text{C}$  NMR ( $\text{CDCl}_3$ ):  $\delta$  144.0, 136.0, 135.7, 129.6, 127.7, 101.4, 71.2, 22.6, 21.3, 4.4. HRMS (ESI)  $m/z$  [ $\text{M} + \text{H}$ ]<sup>+</sup> calcd for  $\text{C}_{12}\text{H}_{15}\text{N}_2\text{O}_2\text{S}$  251.0854, found 251.0856.

**2,4,6-Triisopropylbenzenesulfonylhydrazide ("Trisylhydrazide").**<sup>40</sup> 2,4,6-Triisopropylbenzenesulfonyl chloride (2.05 g, 6.8 mmol) was dissolved in 10 mL THF in a 50 mL, oven-dried round-bottom flask. The solution was cooled to -5 °C, and hydrazine monohydrate (1.3 mL, 26.7 mmol) was added dropwise over 15 min. The solution was stirred at 0 °C for 4 h. Water was added to the solution until the precipitate dissolved, ether was added to form a substantial organic layer, and the aqueous layer was removed. The organic layer was washed 3 times with brine, dried over  $\text{MgSO}_4$ , filtered over a pad of Celite, and concentrated under reduced pressure to afford trisylhydrazide (1.74 g, 5.9 mmol, 86%) as a white solid.  $^1\text{H}$  NMR (300 MHz,  $\text{CDCl}_3$ ):  $\delta$  7.20 (s, 2H), 5.44 (s, br, 1H), 4.15 (sept,  $J = 6.6$  Hz, 2H), 2.92 (sept,  $J = 6.8$  Hz), 1.61 (s, br, 2H), 1.28 (d,  $J = 6.6$  Hz, 12H), 1.26 (d,  $J = 6.8$  Hz, 6H).

**Pent-3-yn-2-one Trisylhydrazone (10).**<sup>41</sup> Trisyl hydrazide (1.56 g, 3.8 mmol) was added to a 100 mL flask containing pent-3-yn-2-one (**8**) (0.32 g, 3.8 mmol), and the flask was purged with nitrogen for 15 min. To this flask was added 23 mL glacial acetic acid, and the reaction was stirred under nitrogen at room temperature for 2 h. The reaction was quenched by pouring the mixture into a large Erlenmeyer flask containing a solution of saturated  $\text{NaHCO}_3$  slowly and stirring for 30 min. The solution was extracted three times with dichloromethane. The combined organic layers were washed with saturated  $\text{NaHCO}_3$  solution, dried over  $\text{MgSO}_4$ , and the pH checked to ensure a neutral solution. The solution was concentrated to reveal a pale yellow solid. The solid was purified by column chromatography ( $\text{SiO}_2$ , 1:5 EtOAc:hexanes) affording pent-3-yn-2-one trisylhydrazone (**10**) (0.80 g, 2.2 mmol, 58%) as a white solid.  $^1\text{H}$  NMR (300 MHz,  $\text{CDCl}_3$ ):  $\delta$  8.28 (s, 1H), 7.16 (s, 2H), 4.21 (sept,  $J = 6.8$  Hz, 2H), 2.90 (sept,  $J = 6.9$  Hz, 1H), 2.10 (s, 3H), 1.99 (s, 3H), 1.27 (d,  $J = 6.8$  Hz, 12H), 1.26 (d,  $J = 6.8$  Hz, 6H). HRMS (ESI-Q-IT)  $m/z$  [ $\text{M} + \text{H}$ ]<sup>+</sup> calcd for  $\text{C}_{20}\text{H}_{31}\text{N}_2\text{O}_2\text{S}$  363.2101, found 363.2097.

**Pent-3-yn-2-one Trisylhydrazone Sodium Salt.** To an oven-dried 25 mL flask, pent-3-yn-2-one trisylhydrazone (**10**) (0.20 g, 0.57 mmol) and NaH (60% in mineral oil) (0.025 g, 0.62 mmol) were added and purged with  $\text{N}_2$  for 15 min. To this was added 9.0 mL distilled diethyl ether, and the suspension was stirred under  $\text{N}_2$  at room temperature. After 90 min, the suspension was filtered, and the precipitate was thoroughly rinsed with hexane. The white solid was dried overnight *in vacuo*.

**2-Diazo-3-pentyne (11).** Pent-3-yn-2-one trisylhydrazone sodium salt (0.15 g, 0.40 mmol) was added to the bottom of an oven-dried sublimator and placed under vacuum. The coldfinger of the sublimator was filled with dry ice/acetone and the bottom of the sublimator was heated to 120 °C. Small pink droplets of 2-diazo-3-pentyne (**11**) began to form on the coldfinger within 5 min. The reaction was allowed to continue for 45 min at which time the coldfinger was removed, and the diazo compound was rinsed into a deposition tube using freshly distilled diethyl ether that had been dried over  $\text{CaH}_2$ . Ether was removed *in vacuo* with the deposition tube cooled to -78 °C to yield 2-diazo-3-pentyne (**11**) a bright pink residue at the bottom of the tube. IR ( $\text{N}_2$ , 10 K) 2965 w, 2928 w, 2901 w, 2860 w, 2199 w, 2067 vs, 2004 w, 1466 w, 1439 m, 1386 m, 1039 w, 664 w  $\text{cm}^{-1}$  (Figure 3); UV/vis ( $\text{N}_2$ , 10 K)  $\lambda_{\text{max}}$  250 nm (Figure S7); UV/vis (MeOH, 298 K)  $\lambda_{\text{max}}$  512, 250 nm (Figure S6).

**Triplet 1,3-Dimethylpropynylidene (**3**).** IR ( $\text{N}_2$ , 10 K) 2931 m, 2897 s, 2830 m, 2725 m, 1443 w, 1429 m, 1369 w, 1311 w, 1002 w  $\text{cm}^{-1}$  (Figure 3); UV/vis ( $\text{N}_2$ , 10 K)  $\lambda_{\text{max}}$  350 nm (Figure 5); EPR (Ar, 10 K)  $|D/hc|$  = major: 0.627 minor: 0.651  $\text{cm}^{-1}$ ,  $|E/hc|$  = major: 0.0073 minor: 0.0048  $\text{cm}^{-1}$ ;  $Z_1$  major: 3240 minor: 3525,  $X_2$  major: 5700

minor: 5885,  $Y_2$  major: 6008 minor: 6092,  $Z_2$  major: 10200 minor: 10400 G; microwave frequency 9.713 GHz (Figure 6).

**Pent-1-en-3-yne (4).**<sup>42</sup> Triethylamine (180 mL) was degassed (nitrogen, 30 min) in a thick-wall pressure tube, and to it was added vinyl bromide (6.0 mL, 85.3 mmol), copper iodide (0.59 g, 3.1 mmol), and bis(triphenylphosphine) palladium(II) dichloride (0.997g, 1.4 mmol). In a separate flask, propyne (8 mL, 106 mmol) was condensed at  $-78$  °C and added via syringe at  $-78$  °C. The pressure tube was sealed with a Teflon screw cap, the cold bath removed, and the mixture stirred at ambient temperature for 18 h. The mixture was first purified by simple distillation. The resulting distillate was then fractionally distilled twice to afford pent-1-en-3-yne (4) with traces of triethylamine. To isolate the pure enyne in deposition glassware, a deposition tube was cooled to  $-78$  °C in liquid  $N_2$  under vacuum, and the sample was opened to the system. The resulting IR spectrum did not show the presence of triethylamine.  $^1H$  NMR (400 MHz,  $CDCl_3$ ):  $\delta$  5.76 (ddq,  $J = 17.5, 11.0, 2.3$  Hz, 1H), 5.55 (dd,  $J = 17.5, 2.2$  Hz, 1H), 5.38 (dd,  $J = 11.0, 2.2$  Hz, 1H), 1.95 (d,  $J = 2.3$  Hz, 3H). IR ( $N_2$ , 10 K) 2976 s, 2925 m, 2862 w, 2341 w, 2241 s, 1848 w, 1716 w, 1613 s, 1598 m, 1443 s, 1415 m, 1387 w, 1295 w, 1170 m, 1071 m, 1028 w, 982 s, 929 s, 680  $w\text{ cm}^{-1}$  (Figure 4).

## ■ ASSOCIATED CONTENT

### Supporting Information

The Supporting Information is available free of charge on the ACS Publications website at DOI: 10.1021/jacs.6b07444.

Experimental and computational details;  $^1H$  and  $^{13}C$  NMR spectra; computed energies, Cartesian coordinates, harmonic vibrational frequencies, and infrared intensities of all species studied at all levels of theory (PDF)

## ■ AUTHOR INFORMATION

### Corresponding Author

\*mcmahon@chem.wisc.edu

### Notes

The authors declare no competing financial interest.

## ■ ACKNOWLEDGMENTS

We gratefully acknowledge financial support from the National Science Foundation (CHE-1011959 and CHE-1362264). We also acknowledge NSF support for Departmental EPR instrumentation (CHE-0741901) and computing facilities (CHE-0840494).

## ■ REFERENCES

- (1) Kaiser, R. I.; Ochsensfeld, C.; Stranges, D.; Head-Gordon, M.; Lee, Y. T. *Faraday Discuss.* **1998**, *109*, 183–204.
- (2) Smith, I. W. M.; Herbst, E.; Chang, Q. *Mon. Not. R. Astron. Soc.* **2004**, *350*, 323–330.
- (3) Miller, J. A.; Klippenstein, S. J. *J. Phys. Chem. A* **2003**, *107*, 2680–2692.
- (4) Taatjes, C. A.; Klippenstein, S. J.; Hansen, N.; Miller, J. A.; Cool, T. A.; Wang, J.; Law, M. E.; Westmoreland, P. R. *J. Phys. Chem. Chem. Phys.* **2005**, *7*, 806–813.
- (5) Seburg, R. A.; DePinto, J. T.; Patterson, E. V.; McMahon, R. J. *J. Am. Chem. Soc.* **1995**, *117*, 835–836.
- (6) Seburg, R. A.; Patterson, E. V.; Stanton, J. F.; McMahon, R. J. *J. Am. Chem. Soc.* **1997**, *119*, 5847–5856.
- (7) Seburg, R. A.; Patterson, E. V.; McMahon, R. J. *J. Am. Chem. Soc.* **2009**, *131*, 9442–9455.
- (8) Osborn, D. L.; Vogelhuber, K. M.; Wren, S. W.; Miller, E. M.; Lu, Y.-J.; Case, A. S.; Sheps, L.; McMahon, R. J.; Stanton, J. F.; Harding, L. B.; Ruscic, B.; Lineberger, W. C. *J. Am. Chem. Soc.* **2014**, *136*, 10361–10372.
- (9) DePinto, J. T.; deProphetis, W. A.; Menke, J. L.; McMahon, R. J. *J. Am. Chem. Soc.* **2007**, *129*, 2308–2315.
- (10) Lee, T. J.; Taylor, P. R. *Int. J. Quantum Chem.* **1989**, *36*, 199–207.
- (11) Lee, T. J. *Chem. Phys. Lett.* **2003**, *372*, 362–367.
- (12) Kassae, M. Z.; Hossaini, Z. S.; Haerizade, B. N.; Sayyed-Alangi, S. Z. *J. Mol. Struct.: THEOCHEM* **2004**, *681*, 129–135.
- (13) Huang, L. C. L.; Lee, H. Y.; Mebel, A. M.; Lin, S. H.; Lee, Y. T.; Kaiser, R. I. *J. Chem. Phys.* **2000**, *113*, 9637–9648.
- (14) Muri, D.; Carreira, E. M. *J. Org. Chem.* **2009**, *74*, 8695–8712.
- (15) Hamed, O.; Henry, P. M.; Becker, D. P. *Tetrahedron Lett.* **2010**, *51*, 3514–3517.
- (16) Seburg, R. A.; Hodges, J. A.; McMahon, R. J. *Helv. Chim. Acta* **2009**, *92*, 1626–1643.
- (17) Bowling, N. P.; Burrmann, N. J.; Halter, R. J.; Hodges, J. A.; McMahon, R. J. *J. Org. Chem.* **2010**, *75*, 6382–6390.
- (18) Thomas, P. S.; Bowling, N. P.; Burrmann, N. J.; McMahon, R. J. *J. Org. Chem.* **2010**, *75*, 6372–6381.
- (19) Bowling, N. P.; Halter, R. J.; Hodges, J. A.; Seburg, R. A.; Thomas, P. S.; Simmons, C. S.; Stanton, J. F.; McMahon, R. J. *J. Am. Chem. Soc.* **2006**, *128*, 3291–3302.
- (20) Shaffer, C. J. Ph.D. Dissertation, University of Wisconsin-Madison, 2010.
- (21) Fan, Q.; Pfeiffer, G. V. *Chem. Phys. Lett.* **1989**, *162*, 472–478.
- (22) Horný, L. u.; Petraco, N. D. K.; Schaefer, H. F. *J. Am. Chem. Soc.* **2002**, *124*, 14716–14720.
- (23) Stanton, J. F. *J. Chem. Phys.* **2007**, *126*, 134309.
- (24) Nimlos, M. R.; Davico, G.; Geise, C. M.; Wenthold, P. G.; Lineberger, W. C.; Blanksby, S. J.; Hadad, C. M.; Petersson, G. A.; Ellison, G. B. *J. Chem. Phys.* **2002**, *117*, 4323–4339.
- (25) Laane, J. In *Structures and Conformations of Non-Rigid Molecules*; Laane, J., Dakkouri, M., van der Veken, B., Oberhammer, H., Eds.; Kluwer: Dordrecht, 1993; pp 65–98.
- (26) Bunker, P. R. *Annu. Rev. Phys. Chem.* **1983**, *34*, 59–75.
- (27) Winnewisser, B. P. In *Molecular Spectroscopy: Modern Research*; Rao, K. N., Ed.; Academic Press: Orlando, 1985; Vol. III, pp 321–419.
- (28) Winnewisser, M.; Winnewisser, B. P.; Medvedev, I. R.; De Lucia, F. C.; Ross, S. C.; Bates, L. M. *J. Mol. Struct.* **2006**, *798*, 1–26.
- (29) Child, M. S. *Adv. Chem. Phys.* **2007**, *136*, 39–94.
- (30) Bernheim, R. A.; Kempf, R. J.; Gramas, J. V.; Skell, P. S. *J. Chem. Phys.* **1965**, *43*, 196–200.
- (31) Bernheim, R. A.; Kempf, R. J.; Reichenbecher, E. F. *J. Magn. Reson.* **1970**, *3*, 5–9.
- (32) Kaiser, R. I.; Mebel, A. M.; Lee, Y. T.; Chang, A. H. H. *J. Chem. Phys.* **2001**, *115*, 5117–5125.
- (33) Cremer, D.; Kraka, E.; Joo, H.; Stearns, J. A.; Zwier, T. S. *Phys. Chem. Chem. Phys.* **2006**, *8*, 5304–5316.
- (34) Thomas, P. S.; Bowling, N. P.; McMahon, R. J. *J. Am. Chem. Soc.* **2009**, *131*, 8649–8659.
- (35) Gerson, F.; Huber, W. In *Electron Spin Resonance Spectroscopy of Organic Radicals*; Wiley-VCH Verlag: Weinheim, 2003; pp 49–82.
- (36) Frisch, M. J.; Trucks, G. W.; Schlegel, H. B.; Scuseria, G. E.; Robb, M. A.; Cheeseman, J. R.; Scalmani, G.; Barone, V.; Mennucci, B.; Petersson, G. A.; Nakatsuji, H.; Caricato, M.; Li, X.; Hratchian, H. P.; Izmaylov, A. F.; Bloino, J.; Zheng, G.; Sonnenberg, J. L.; Hada, M.; Ehara, M.; Toyota, K.; Fukuda, R.; Hasegawa, J.; Ishida, M.; Nakajima, T.; Honda, Y.; Kitao, O.; Nakai, H.; Vreven, T.; Montgomery, J. A., Jr.; Peralta, J. E.; Ogliaro, F.; Bearpark, M.; Heyd, J. J.; Brothers, E.; Kudin, K. N.; Staroverov, V. N.; Kobayashi, R.; Normand, J.; Raghavachari, K.; Rendell, A.; Burant, J. C.; Iyengar, S. S.; Tomasi, J.; Cossi, M.; Rega, N.; Millam, J. M.; Klene, M.; Knox, J. E.; Cross, J. B.; Bakken, V.; Adamo, C.; Jaramillo, J.; Gomperts, R.; Stratmann, R. E.; Yazyev, O.; Austin, A. J.; Cammi, R.; Pomelli, C.; Ochterski, J. W.; Martin, R. L.; Morokuma, K.; Zakrzewski, V. G.; Voth, G. A.; Salvador, P.; Dannenberg, J. J.; Dapprich, S.; Daniels, A. D.; Farkas, O.; Foresman, J. B.; Ortiz, J. V.; Cioslowski, J.; Fox, D. J. *Gaussian 09*, revision B.1; Gaussian, Inc.: Wallingford, CT, 2009.
- (37) Stanton, J. F.; Gauss, J.; Harding, M. E.; Szalay, P. G. *CFOUR, Coupled-Cluster Techniques for Computational Chemistry*; with contributions from Auer, A. A.; Bartlett, R. J.; Benedikt, U.; Berger, C.; Bernholdt, D. E.; Bomble, Y. J.; Cheng, L.; Christiansen, O.; Heckert,



M.; Heun, O.; Huber, C.; Jagau, T.-C.; Jonsson, D.; J., Jusélius, Klein, K.; Lauderdale, W. J.; Matthews, D. A.; Metzroth, T.; D. P., O'Neill, Price, D. R.; Prochnow, E.; Ruud, K.; Schiffmann, F.; Schwalbach, W.; Stopkowicz, S.; Tajti, A.; J., Vázquez, Wang, F.; Watts, J. D. and the integral packages: MOLECULE (J., Almlöf, Taylor, P. R.), PROPS (Taylor, P. R.), ABACUS (Helgaker, T.; H. J. Aa., Jensen, Jørgensen, P., Olsen, J.), and ECP routines by Mitin, A. V.; C., van Wüllen; [www.cfour.de](http://www.cfour.de).

(38) Glendening, E. D.; Badenhop, J. K.; Reed, A. E.; Carpenter, J. E.; Bohmann, J. A.; Morales, C. M.; Landis, C. R.; Weinhold, F. *NBO 6.0 Theoretical Chemistry Institute*; University of Wisconsin-Madison: Madison, WI, 2013.

(39) Coleman, R. S.; Lu, X.; Modolo, I. *J. Am. Chem. Soc.* **2007**, *129*, 3826–3827.

(40) Pattabiraman, V. R.; Stymiest, J. L.; Derksen, D. J.; Martin, N. I.; Vederas, J. C. *Org. Lett.* **2007**, *9*, 699–702.

(41) Kirmse, W.; Heese, J. *J. Chem. Soc. D* **1971**, 258–259.

(42) Brewitz, L.; Llaveria, J.; Yada, A.; Fürstner, A. *Chem. - Eur. J.* **2013**, *19*, 4532–4537.